Contr. Mineral. and Petrol. 20, 203—234 (1969)

Shock Induced Planar Deformation Structures in Quartz from the Ries Crater, Germany

W. v. Engelhardt and W. Bertsch
Mineralogisches Institut der Universität Tübingen

Received October 31, 1968

Abstract. Crystalline rocks from breccias of the Ries basin, Germany, contain highly deformed quartz. Various planar deformation structures could be observed and classified into five different types: (1) Decorated planar elements, (2) Non-decorated planar elements, (3) Homogeneous lamellae, (4) Filled lamellae, (5) Planar fractures. All these structures are parallel to crystallographic planes: {10$\bar{1}$3}, {10$\bar{1}$2}, {10$\bar{1}$1}, {0001}, {11$\bar{2}$1}, {11$\bar{2}$2}, 21$\bar{3}$1}, {51$\bar{6}$1}, {10$\bar{1}$0}. The most typical and most abundant planar structures are decorated and non-decorated planar elements parallel to {10$\bar{1}$3} and {10$\bar{1}$2}. Planar fractures are parallel to {0001} and {10$\bar{1}$1} and form at lower stress levels, probably earlier than the planar elements.

Quartz containing planar elements, especially of the non-decorated type, has lower density, index of refraction and birefringence than normal quartz. This "quartz" is apparently a mixture of an amorphous phase and crystalline quartz, the amount of which can be calculated using average density or refractive index.

Comparison of planar quartz structures found in tectonites and those produced artificially under static or dynamic high pressure conditions demonstrates that Ries quartz closely resembles deformed quartz recovered from shock wave experiments. The planar structures found in Ries quartz have been formed by shock wave actions with peak pressures in the 100—400 kbar range.

Planar elements are explained to be traces of gliding processes during shock loading visible due to the fact that a high pressure phase (stishovite and/or a stishovite-like glass phase) has been produced along the glide planes. Upon pressure release most of the high pressure phase was transformed into an SiO_2-glass (diaplectic glass).

In comparison with experimental data the amount of residual crystalline quartz as well as type and orientation of planar structures in the quartz grains are clues to estimate the peak pressures responsible for these deformations. Shock waves with peak pressures exceeding about 400 kbar completely transform quartz into diaplectic SiO_2-glass.

Contents

1. Introduction

Planar deformation structures in quartz have been observed in brecciated rocks from many craters of suspected meteorite impact origin (McIntire, 1962; Bunch and Cohen, 1964; Dence, 1964; Dence, 1965; Engelhardt and Stöffler, 1965; Stöffler, 1966; Chao, 1967; Engelhardt, 1967; Engelhardt, Bertsch, Stöffler, Groschopf, and Reiff, 1967; Chao, 1968; Robertson, Dence and Vos, 1968; Engelhardt, Hörz, Stöffler and Bertsch, 1968; Carter, 1968; French, 1967). Several types of planar structures have been described using different terms such as deformation lamellae, planar features and cleavages. All types seem to be more or less different from deformation structures in quartz known from tectonites or artificially produced in low strain rate experiments. Deformation structures more similar to those from meteorite craters, however, have been found in shock loaded rocks from nuclear explosion sites (Short, 1966). Recently they also have been produced in shock wave experiments of known peak pressure (Short, 1968c; Hörz, 1968; Müller and Defourneaux, 1968). Thus planar deformation structures in quartz developed to be a diagnostic criterion for shock wave action. They can be used to identify and distinguish meteoritic impact craters from volcanic structures on earth or other planetary bodies.

This paper presents a description of quartz with planar structures, collected in various breccias of the Ries basin. In addition, these types of planar structures are compared to deformation structures found in tectonites (Böhm lamellae) and those produced in the laboratory under low and high strain rates (static and dynamic conditions). The investigations in naturally shocked materials are restricted to 12 rock samples representative for shock metamorphism stages I and II. These samples were selected out of a large suite of rocks for detailed studies. No attempt is made to compare this quartz with quartz from other craters (see, e.g., the description of quartz deformation in Canadian craters by Robertson, Dence and Vos, 1968). This would imply a careful consideration of all geological and petrographic parameters and thereby exceed the scope of this article. However, the types of deformation structures found in the Ries are also commonly observed in other craters and the following description may be more general in its nature.

2. Petrography of the Investigated Rocks

Quartz with planar deformation structures is found in various breccias of the Ries (for a general description of Ries rocks see Preuss, 1964; Engelhardt, 1967): they could be identified qualitatively in the suevite, in the crystalline

Table 1. *Petrography of investigated rock samples. All rocks contain apatite, zircon and opaques as minor constituents, S 350 and B 41 secondary calcite.* $\bar{n}$ *is the average refractive index of the diaplectic quartzes and glasses, see Table 8. % are volume percentages*

No.	Rock name	Stage of shock metamorphism	Quartz vol. percentage, grain size and refractive index	Feldspar	Biotite	Amphibole
B 10	quartz diorite gneiss	I	33% [0.05—0.5 mm] $\bar{n} = 1.546$	61% oligoclase	5%	—
B 51	granite gneiss	I	32% [0.05—0.4 mm] $\bar{n} = 1.546$	63% oligoclase and orthoclase	5%	—
S 289	granite or quartz diorite gneiss	II	19% [0.1 —0.8 mm] $\bar{n} = 1.545$	57% feldspar, nearly completely isotropic	24% with kinkbands	—
B 36	granite	I	33% [0.2 —1.0 mm]	64% oligoclase and orthoclase, the latter with sanidine optics	3%	—
B 151	diorite	II	6% [0.05—0.4 mm] $\bar{n} = 1.536$	47% oligoclase-andesine. Isotropic twin lamellae	12%	35% with twin lamellae
B 1	quartz diorite gneiss	II	33% [0.2 —0.6 mm] $\bar{n} = 1.534$	62% oligoclase. Isotropic twin lamellae	3%	1%
S 350	granite or diorite gneiss	II	34% [0.2 —0.1 mm] $\bar{n} = 1.533$	60% feldspar partially or completely isotropic	5% biotite and chlorite	—
S 349	quartz diorite gneiss	II	22% [0.6 —0.2 mm] $\bar{n} = 1.529$	55% andesine, partially or completely isotropic (see STÖFFLER, 1967)	4% with kinkbands	19%
B 7	granite or quartz diorite gneiss	II	37% [0.2 —0.6 mm] $\bar{n} = 1.480$ partially isotropic and transformed into secondary clay minerals	58% feldspar Partially isotropic, recrystallisation	4%	—
B 9	granite or quartz diorite gneiss	II	35% [0.2 —0.8 mm] $\bar{n} = 1.479$ partially transformed into secondary clay minerals	60% feldspar, partially isotropic, recrystallisation	4%	—

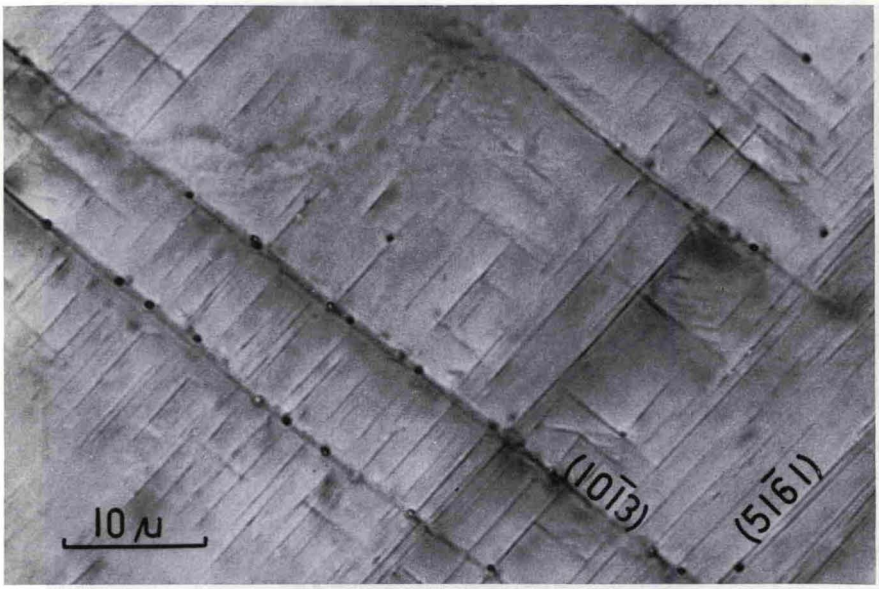

Fig. 2. Planar elements with some single decorations in quartz from sample B 151. Plane polarized light

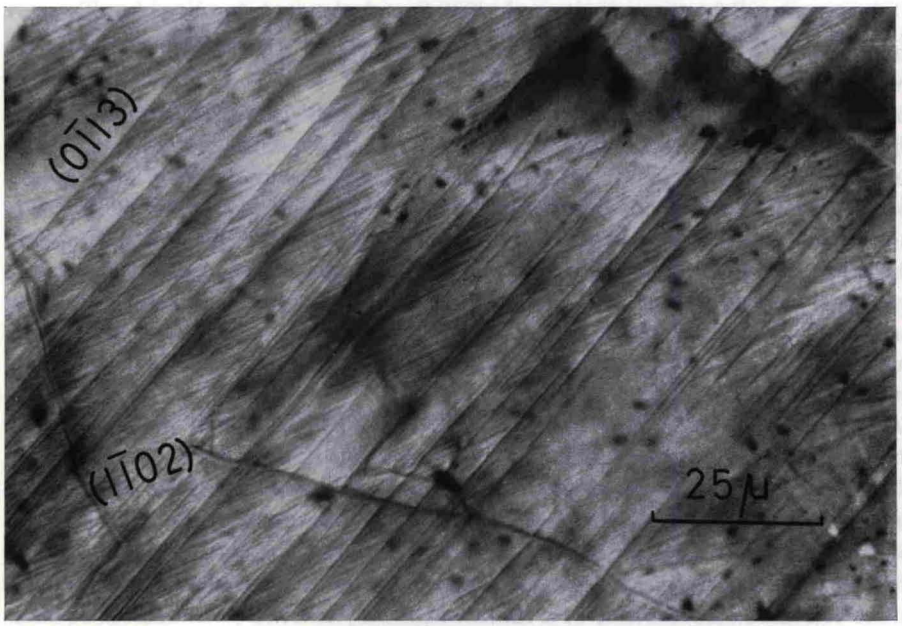

Fig. 3. Non-decorated planar elements in quartz from sample B 7. Crossed nicols

found in the sample S 349 (Fig. 4). Some lamellae can be observed only under highest magnifications (oil immersion).

All quartz lamellae in the investigated rock samples are symmetrical. Asymmetric lamellae like those reported by Christie, Griggs and Carter (1964) from studies

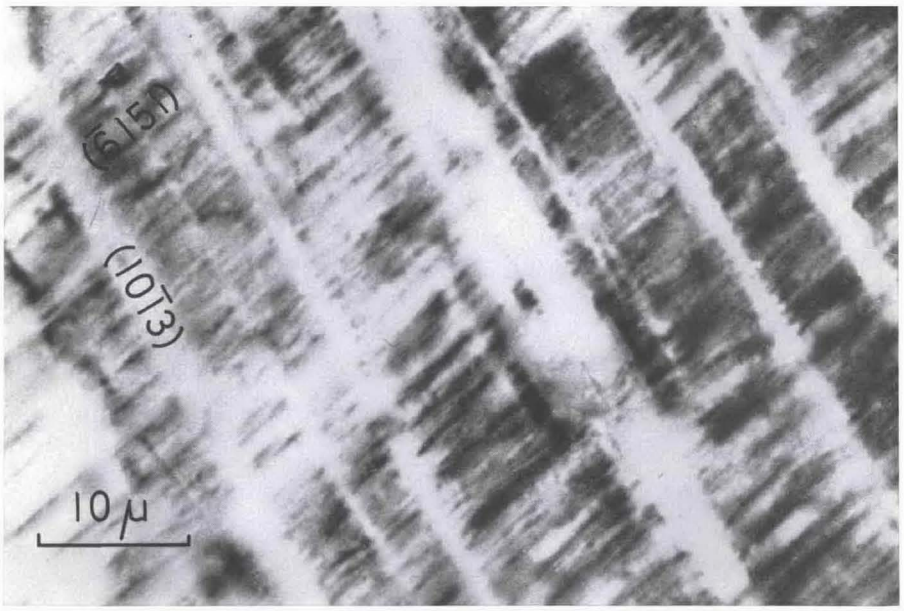

Fig. 4. Homogeneous lamellae in quartz from sample S 349. Crossed nicols

of quartz samples compressed under static high pressure conditions as well as CARTER (1964, 1968) from several impact crater breccias have not been found. In our samples asymmetrical effects are sometimes observed, both in normal or phase contrast illumination, due to an oblique cut of the planar elements.
Differences in extinction of lamellae and surrounding quartz range between 0° and 5°. Phase contrast illumination reveals very clearly that the refractive indices of the lamellae are lower that those of the host quartz. Also their birefringence is lowered. Most lamellae of this kind are parallel to {10$\bar{1}$3} planes.
3.1.4. Filled Lamellae. Multiple sets of these lamellae parallel to {10$\bar{1}$3} planes have only been found in sample S 289 (Fig. 5). They are 1 to 3 μ thick, of lenticular shape and filled with very fine crystalline material of higher refractive index and higher birefringence than the host quartz.
Since sample S 289 contains stishovite (STÖFFLER, personal communication) it is assumed that the granular material filling the lamellae is stishovite.
3.1.5. Planar Fractures. Quartz in all investigated samples contains planar fractures parallel to rational crystallographic orientations. The broadest of these appear as open fissures filled with secondary minerals such as montmorillonite or quartz. They are not as abundant as decorated and smooth planar elements nor are they arranged in the same regular manner. In addition, their spacing is much wider (mutual distance more than 20 μ). Planar fractures of this type occur preferably parallel to {0001} or {10$\bar{1}$1}, some few parallel to {10$\bar{1}$3}.
Figs. 6 and 7 illustrate examples of planar fractures parallel to {0001} and {10$\bar{1}$1}. It can be seen that these fractures first broke the quartz grains into separate parts. In a later stage closely spaced planar elements developed confined to these individual domains. Planar fractures acted like grain boundaries and were not

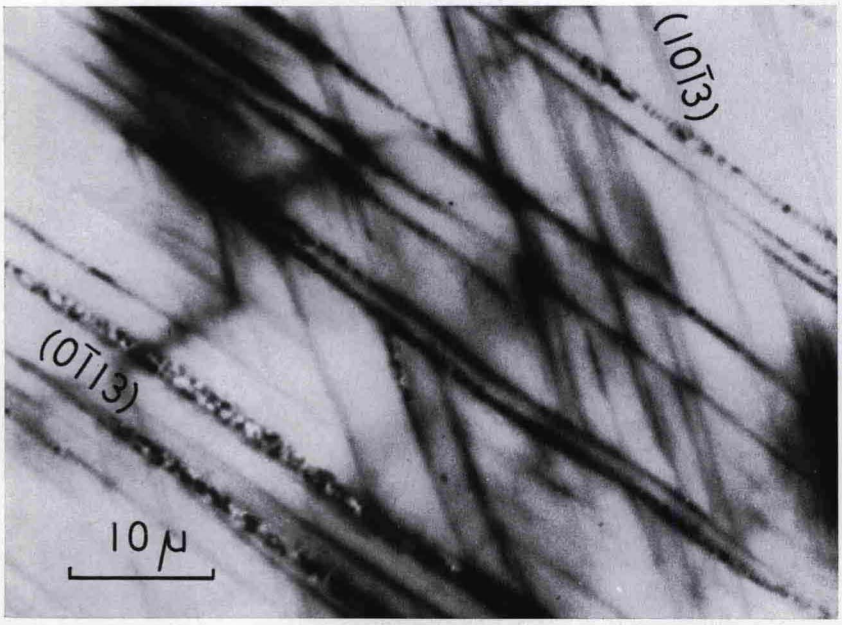

Fig. 5. Lamellae filled with fine grained stishovite. Quartz from sample S 289. Crossed nicols

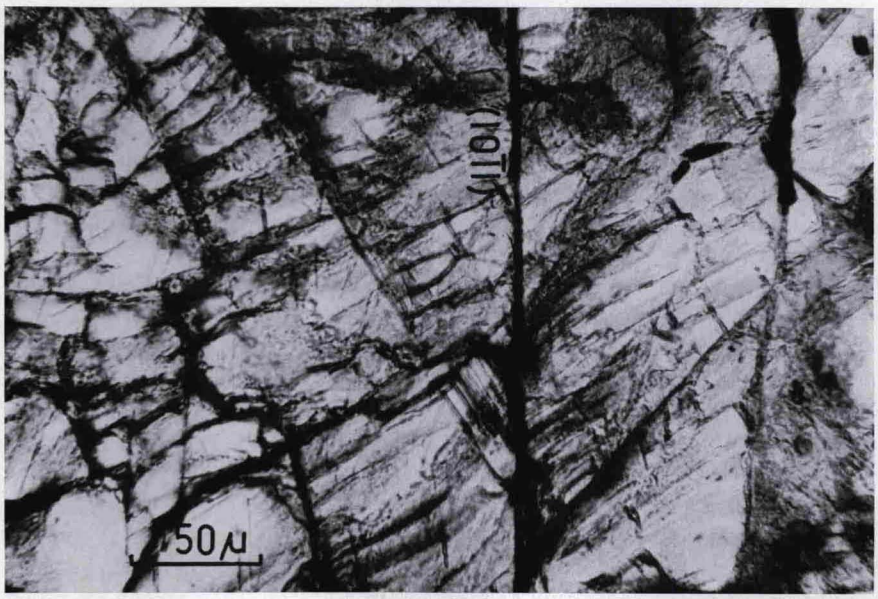

Fig. 6. Planar fracture parallel to {10$\bar{1}$1} and planar elements parallel to {10$\bar{1}$3}, formed later, therefore terminating at the fracture. Quartz from sample S 350. Crossed nicols

transgressed by planar elements. In cases like those illustrated in Figs. 6 and 7 the difference of planar elements and planar fractures is readily seen. Their distinction becomes difficult however — sometimes even impossible — if the planar fractures

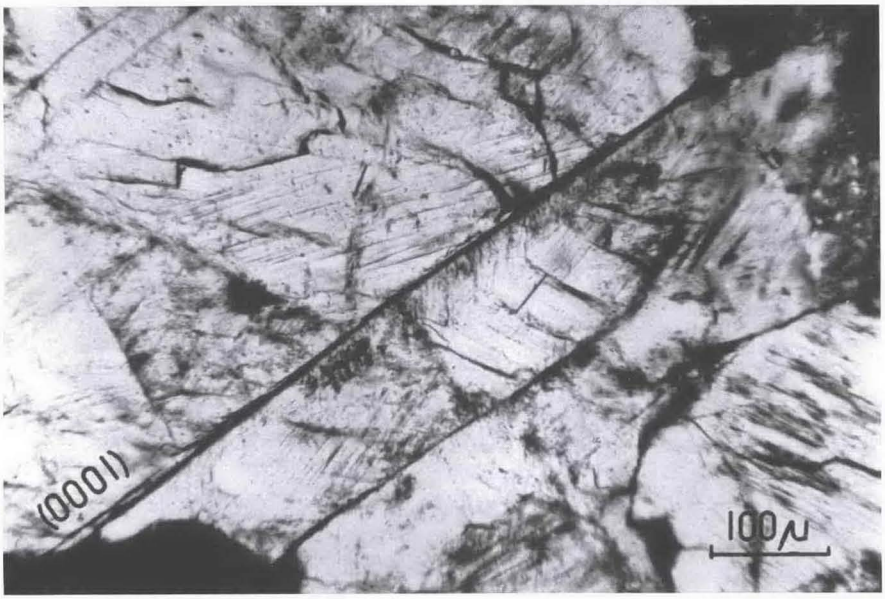

Fig. 7. Planar fracture parallel to {0001} and planar elements parallel to {10$\bar{1}$3}, formed later therefore terminating at the fracture. Quartz from sample S 350

are not open fissures. Regardless of their nature, smooth planar elements are discontinuity planes and zones of weakness. It has been demonstrated that quartz from a breccia of West Clearwater Lake, Canada, containing many planar elements of the non-decorated type breaks preferentially parallel to these features (Engelhardt, Hörz, Stöffler, Bertsch, 1968). The same holds true for quartz from the Ries. An example is shown in Fig. 8. Under natural or artificial stress, quartz with non-decorated planar elements can break into platelets parallel to the planes of these elements. But fractures of this nature are always formed later than the planar elements, unlike the type of planar fractures mentioned above.

Since the multiple sets of smooth planar elements resemble strikingly cleavage patterns and additionally quartz containing such elements has the tendency to break along these planes, the non-decorated planar deformation structures from the Ries and Lake Mien, Sweden, have initially been reported as "cleavages" (Engelhardt and Stöffler, 1965). We now recommend to avoid the term "cleavage" in this connection. Cleavage means a perfect straight fracture producible potentially along all planes parallel to a certain rational plane of the undisturbed lattice. However, partition along non-decorated planar elements as observed in quartz from the Ries and other craters is due to a weakening of cohesion of the grains in these planes, produced under extraordinary stress conditions.

3.2. Crystallographic Orientation

The orientations of all five types of planar structures as defined in the last sections and their angular relation to the optic axes were measured with standard universal

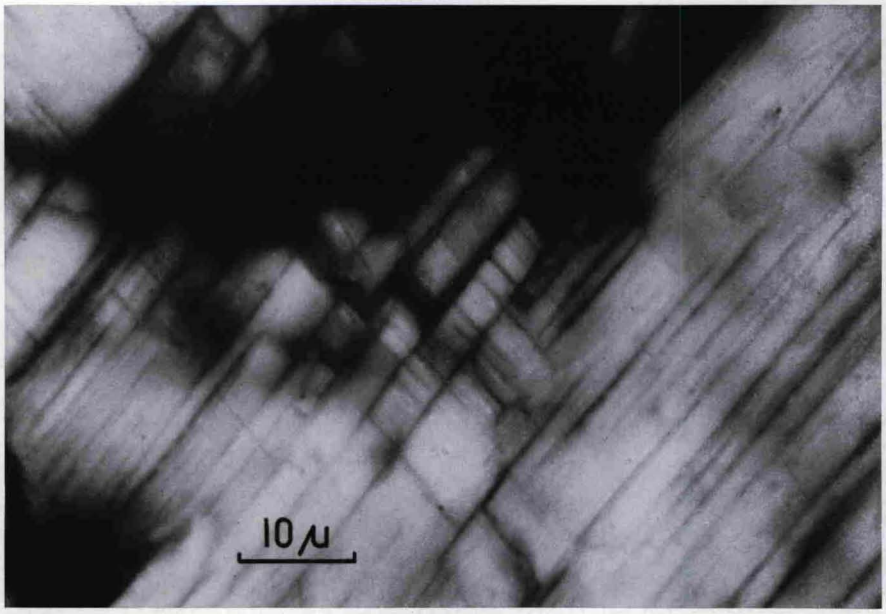

Fig. 8. Fracturing, caused during thin section preparation, following planar elements parallel to $\{10\bar{1}3\}$. Quartz from sample B 51. Crossed nicols

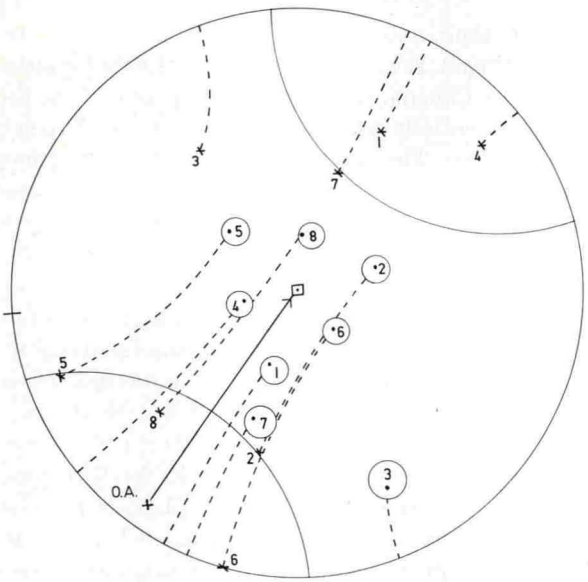

Fig. 9. Determination of the crystallographic orientation of planar structures. Stereographic projection. *Crosses*: Poles of planar elements (actual measurements on the U-stage). *OA*: Optic axis (actual measurements on the U-stage). The small circles represent the "blind" circle after rotation. *Points*: Poles of planar elements after transformation of the optic axis into the center of projection. 4, 6, 8: $\{10\bar{1}3\}$ or $\{01\bar{1}3\}$; 1, 2, 5: $\{01\bar{1}2\}$ or $\{10\bar{1}2\}$; 3: $\{21\bar{3}1\}$; 7: $\{10\bar{1}1\}$

stage techniques using thin sections. Per each grain the position of the optic axis and the poles of all measurable planar structures were plotted in individual stereo plots. An example is shown in Fig. 9. This particular grain displayed eight different sets of planar structures. The "blind circle" encloses the area not accessible to observation using an universal stage. The crosses indicate the actual measurements

of poles and optic axis, the center of the plot being the normal to the thin section. All projections were then normalized by rotating the optic axis into the center. The new positions of the poles — resulting from this rotation — are indicated by circles. This standard projection allows the identification of the poles of planar elements with crystallographic planes. By definition a pole was assumed to coincide with a crystallographic plane if the angle between measured and ideal plane differed less than 5°. This allowance corresponds to the accuracy of universal stage measurements. This method allows a more precise identification of planar

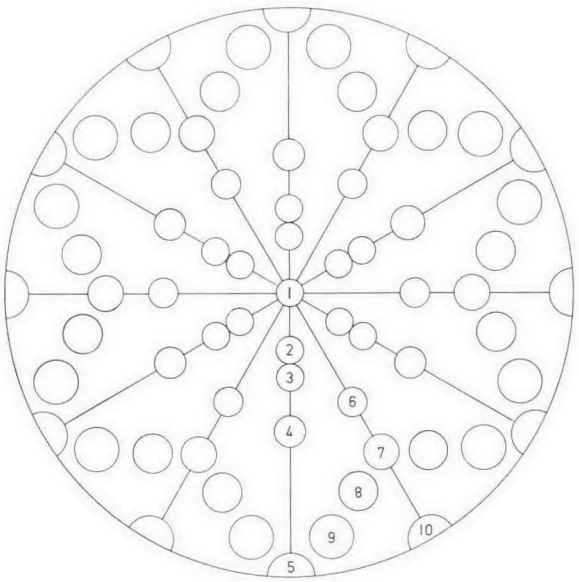

Fig. 10. Crystallographic orientation of the observed planar structures. Angles between poles of planes and optic axis:
1. (0001): 0°
2. $(10\bar{1}3)$: 22°56'
3. $(10\bar{1}2)$: 32°25'
4. $(10\bar{1}1)$: 51°47'
5. $(10\bar{1}0)$: 90°
6. $(11\bar{2}2)$: 47°43'
7. $(11\bar{2}1)$: 65°33'
8. $(21\bar{3}1)$: 73°25'
9. $(51\bar{6}1)$: 81°57'
10. $(11\bar{2}0)$: 90°

structures with low index planes as compared to measurements of their angle to the optic axis alone, the method commonly used by various authors. The orientation of all planar structures investigated is shown in Fig. 10. The diameters of the circles correspond to the 5° accuracy of the measurements.

Approximately 50 grains have been measured per each thin section. On the average 3 to 10 different sets of planar structures per grain were observed with a maximum of 18 sets for a single grain.

Qualitative frequencies concerning the various types of deformation structures are given in Table 2. Quantitative frequencies of all features combined are listed in Tables 3 and 4 and illustrated in Figs. 10 and 11.

The following parameters have been reduced from the microscopical data:

q_{hkil} = actual number of symmetrically equivalent deformation planes $\{hkil\}$ observed in n quartz grains.

p_{hkil} = maximum number of symmetrically equivalent planes $\{hkil\}$ potentially observable in n quartz grains, accounting for the limitations of grain orientation and blind circle.

Q = total number of all sets of planar structures observed in n quartz grains.

Table 2. *Qualitative frequencies of planar deformation structures in quartz of the investigated rock samples*

No. of rock sample	Planar structures					Irregular fractures
	decorated planar elements	non-decorated planar elements	homogeneous lamellae	filled lamellae	planar fractures	
B 10	some	few	—	—	some	very many
B 51	many	few	very few	—	some	very many
S 289	—	many	—	very many	some	many
B 36	very many	few	many	—	some	many
B 151	many	many	some	—	some	some
B 1	many	many	few	—	some	many
S 350	many	many	some	—	some	some
S 349	many	very many	some	—	some	some
B 7	—	very many	very few	—	some	few
B 9	—	very many	very few	—	some	some

Table 3. *Relative frequencies f_{hkil} (%) of planar structures in quartz from Ries rocks*

Sample No.	B 10	B 51	S 289	B 36	B 151	B 1	S 350	S 349	B 7	B 9
{0001}	21	20	0	22	2	57	33	2	9	13
{10$\bar{1}$3}	44	53	60	52	66	53	68	55	51	63
{10$\bar{1}$2}	0.5	1	31	31	32	34	59	45	52	49
{10$\bar{1}$1}	3	6	18	19	30	33	40	26	6	27
{11$\bar{2}$2}	1	3	3	6	5	8	1	6	4	5
{11$\bar{2}$1}	0.3	1	5	3	4	7	3	8	6	4
{21$\bar{3}$1}	1	2	4	6	7	9	7	7	6	7
{51$\bar{6}$1}	1	2	4	3	4	5	2	5	3	4
{10$\bar{1}$0} {11$\bar{2}$0}	1	2	2	4	6	12	6	8	4	8
Sets per grain	2.8	4	6.7	7.3	9	11	10	8.8	7.6	9.2

Table 4. *Absolute frequencies F_{hkil} (%) of planar structures in quartz from Ries rocks*

Sample No:	B 10	B 51	S 289	B 36	B 151	B 1	S 350	S 349	B 7	B 9
{0001}	6	5	0	3	0.2	5	3	0.2	1	1
{10$\bar{1}$3}	75	70	44	38	42	29	34	33	38	37
{10$\bar{1}$2}	1	2	22	22	19	17	30	25	36	27
{10$\bar{1}$1}	6	7	13	12	16	15	20	14	4	14
{11$\bar{2}$2}	2	4	2	4	3	4	0.3	3	3	2
{11$\bar{2}$1}	0.5	1	4	2	2	3	1	4	3	2
{21$\bar{3}$1}	2	3	6	8	7	8	7	6	7	8
{51$\bar{6}$1}	4	4	5	4	4	5	2	5	4	4
{10$\bar{1}$0} {11$\bar{2}$0}	2	2	2	3	3	5	3	4	2	4
Not identified:	1.4	3	3	4	4	11	0.6	6	3	1.3

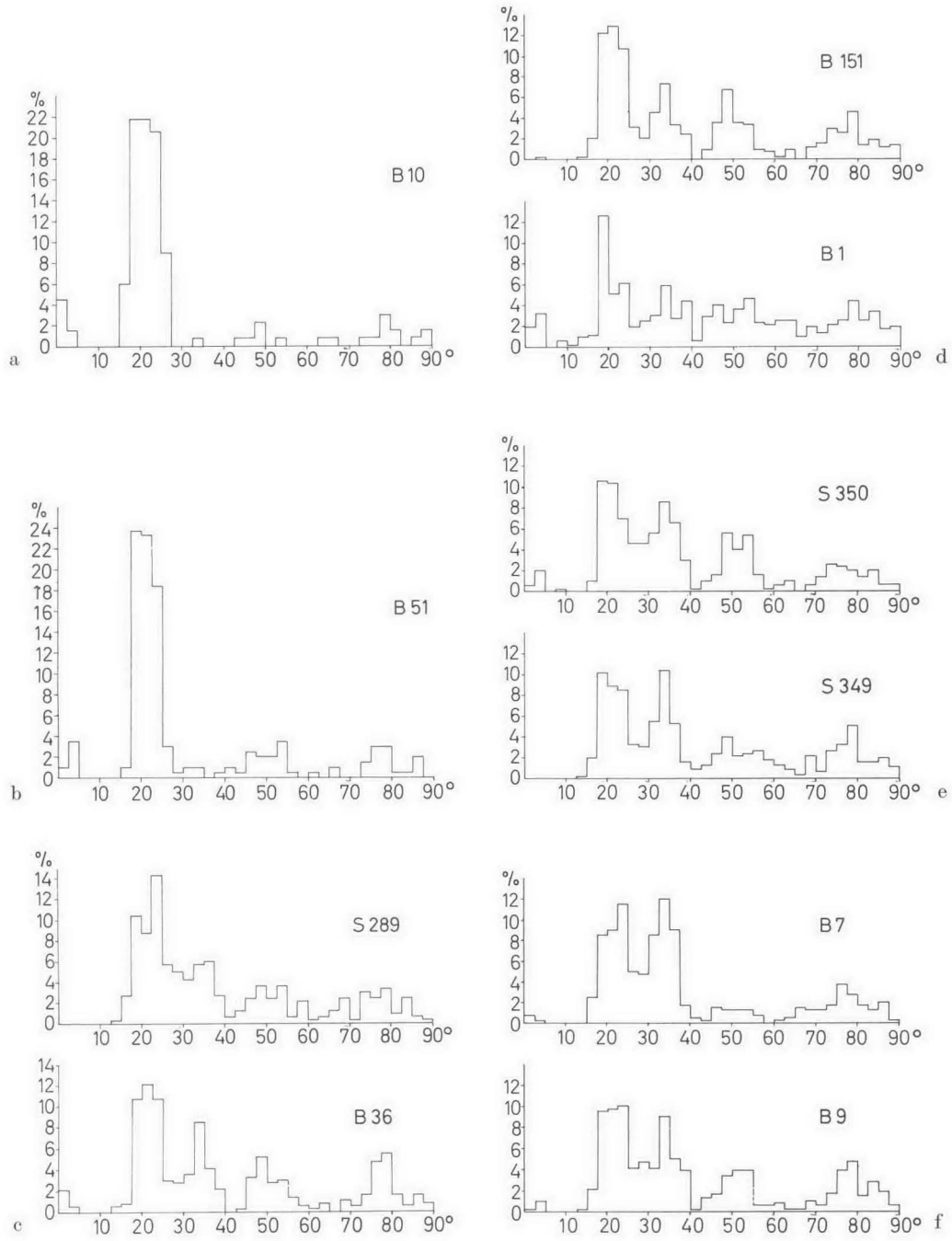

Fig. 11. Frequency distribution of measured angles between poles of planar structures and optic axis

Using these definitions, relative (f_{hkil}) and absolute F_{hkil}) frequencies were calculated. They are recorded in Tables 3 and 4.

$$\text{relative frequency:} \quad f_{hkil} = \frac{q_{hkil}}{p_{hkil}} \cdot 100\,(\%)$$

$$\text{absolute frequency:} \quad F_{hkil} = \frac{q_{hkil}}{Q} \cdot 100\,(\%).$$

For better comparison of our results with data published elsewhere the more familiar plots of the angles between poles of planar features and the optic are shown in Fig. 11.

3.3. Spatial Distribution within the Grains

Within an individual quartz grain, the distribution of planar elements and lamellae is not necessarily uniform. Quite often they concentrate near grain boundaries in particular in corners. Sometimes a certain part of the grain does not display any planar elements or lamellae at all.

In single grains — positioned suitably — one can determine how many symmetrically equivalent planes exclusively of the same positive or negative crystallographic form do exist, or whether the features present are combinations of both. Table 5 lists the results of these observations for decorated and non-decorated planar elements parallel to $\{10\bar{1}3\}$, respectively $\{01\bar{1}3\}$. Only those quartz grains were used in which all 3 positive and all three negative rhombohedra could be observed potentially ($p_{hkil} = 6n$; $n = 30$). The figures give the percentage of grains in which the combination in question was observed: for instance all three rhombohedron faces of one form, either $\{10\bar{1}3\}$ or $\{01\bar{1}3\}$, could be observed in 16% of all quartz grains of B 151.

Table 5. *Combinations of planar structures parallel to $(10\bar{1}3)$ and/or $(01\bar{1}3)$ in single quartz grains. The figures give the percentage of grains in which a particular combination was observed*

Rhombohedra $(10\bar{1}3)$ and $(01\bar{1}3)$	B 10	B 51	S 289	B 36	B 151	B 1	S 350	S 349	B 7	B 9
3 positive and 3 negative	3	6	15	13	18	9	27	3	3	10
3 positive and 2 negative or vice versa	3	3	12	8	29	14	9	16	8	10
3 positive and 1 negative or vice versa	3	18	8	8	13	17	5	21	8	17
3 positive or 3 negative	19	29	8	32	16	34	41	26	29	53
2 positive and 2 negative	6	9	19	—	5	6	9	8	11	—
2 positive and 1 negative or vice versa	13	18	8	3	8	3	5	8	18	3
2 positive or 2 negative	19	6	12	13	5	11	5	16	18	7
1 positive and 1 negative	6	—	15	8	3	6	—	3	3	—
1 positive or 1 negative	19	6	—	13	3	—	—	—	—	—
none	6	6	4	—	—	—	—	—	3	—

In most specimens however there was a tendency for only one rhombohedron to develop in an individual grain, either the positive or negative one. It may be that some of the quartz which seem to contain corresponding forms of opposite signs are actually twinned, each twin developing its own form.

Similar observations can be made using $\{10\bar{1}2\}$ and $\{01\bar{1}2\}$ or $\{10\bar{1}1\}$ and $\{01\bar{1}1\}$ faces. However due to the blind circle, the number of grains in which all 6 planes of these steeper rhombohedra are observable is much more restricted. Good statistics are not readily obtained.

In grains with sets parallel to all three rhombohedra, it is common that $\{10\bar{1}3\}$ (or $\{01\bar{1}3\}$) is combined with $\{01\bar{1}2\}$ (or $\{10\bar{1}2\}$) and $\{10\bar{1}1\}$ (or $\{01\bar{1}1\}$). If various crystallographic forms coexist positive and negative forms tend to alternate (with increasing inclination to c).

Table 6 shows the percentage of quartz grains containing sets of planar structures parallel to identical planes. $\{10\bar{1}3\}$ or $\{01\bar{1}3\}$ occurs in more than 80% of all grains The most frequent combinations are the rhombohedra $\{10\bar{1}3\}$ (or $\{01\bar{1}3\}$), $\{10\bar{1}2\}$ (or $\{01\bar{1}2\}$) and $\{10\bar{1}1\}$ (or $\{01\bar{1}1\}$), often coexisting with the trapezohedron $\{21\bar{3}1\}$.

Table 6. *Frequency of planar structures parallel to different planes. The figures represent the percentage of quartz grains containing planar structures parallel to a particular crystallographic plane (hkil), including all equivalent forms*

Sample No.	B 10	B 51	S 289	B 36	B 151	B 1	S 350	S 349	B 7	B 9
$\{0001\}$	17	18	—	20	2	57	27	2	9	12
$\{10\bar{1}3\}$	92	90	94	96	98	92	87	98	96	94
$\{10\bar{1}2\}$	3	8	62	84	72	81	93	98	93	94
$\{10\bar{1}1\}$	13	26	58	58	70	84	77	75	25	66
$\{11\bar{2}2\}$	4	16	14	24	20	33	3	23	18	16
$\{11\bar{2}1\}$	1	4	20	14	18	24	13	29	20	16
$\{21\bar{3}1\}$	5	12	26	48	58	57	57	58	48	64
$\{51\bar{6}1\}$	8	8	22	18	30	31	13	31	20	26
$\{10\bar{1}0\}$ / $\{11\bar{2}0\}$	4	8	12	16	24	37	23	27	14	32

Sometimes a historic sequence of formation can be observed for sets with different orientation: in most cases $\{10\bar{1}3\}$ or $\{01\bar{1}3\}$ structures are strongly developed spreading evenly almost over the entire grain. Their interspace is filled with more closely spaced elements parallel to $\{10\bar{1}2\}$ or $\{01\bar{1}2\}$ thus indicating a later generation. An example is shown in Fig. 12.

In most cases planar structures parallel to $\{0001\}$ and $\{10\bar{1}1\}$ or $\{01\bar{1}1\}$ seem to have formed prior to $\{10\bar{1}3\}$ or other forms.

Even within correlate forms sometimes a difference in time of formation exists: Fig. 5 shows planar elements parallel to $\{10\bar{1}3\}$ (or $\{01\bar{1}3\}$) apparently older than those parallel to $\{01\bar{1}2\}$ (or $\{10\bar{1}2\}$).

In quartz containing smaller amounts of planar structures the width between the numerous individual planes of one set is rather irregular. Frequently two or three planes are close to each other, separated from the next cluster by a broader interval, void of planar elements: see Fig. 13. Quartz grains with the highest

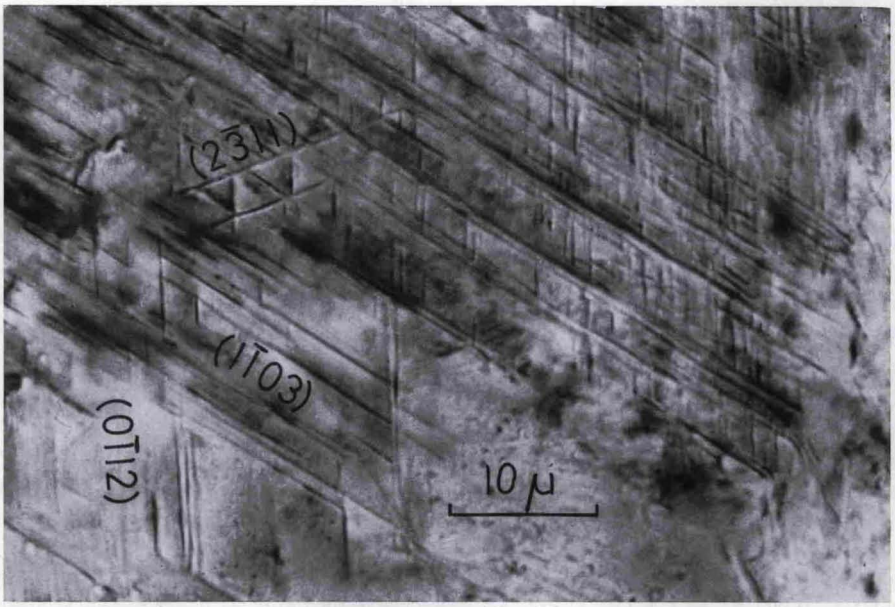

Fig. 12. Non-decorated planar elements parallel to {10$\bar{1}$2}, probably formed later than those parallel to {10$\bar{1}$3}. Quartz from sample S 350. Plane polarized light

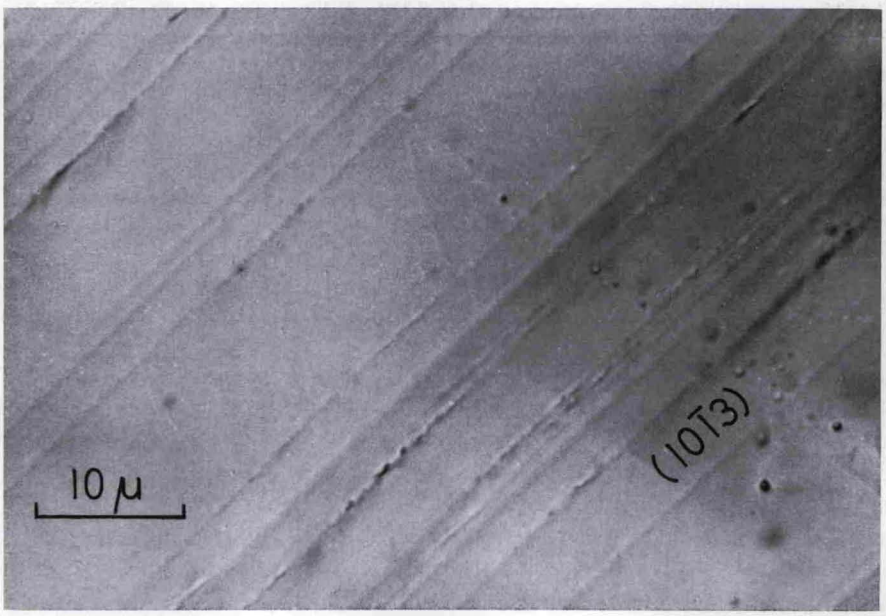

Fig. 13. Irregular distances within multiple sets of planar elements parallel to {10$\bar{1}$3}. Quartz from sample B 10. Crossed nicols

concentrations of planar structures (B 7 and B 9, see Figs. 3 and 16) display a very regular spacing of the planar elements. The individuals are so closely packed that measurement of their orientation becomes increasingly difficult.

Table 7. *Distances of individual elements within multiple sets of planar structures in μ. (Averages and standard deviations)*

	B 10	B 51	S 289	B 36	B 151	B 1	S 350	S 349	B 7	B 9
{0001}	12.5 ± 5.9	23.5 ± 14	—	16.8 ± 6.7	—	22.0 ± 7.2	19.0 ± 7.2	—	31.5 ± 22	22.5 ± 9.0
{10$\bar{1}$3} and {01$\bar{1}$3}	7.8 ± 2.0	8.6 ± 2.6	7.8 ± 1.9	7.4 ± 1.4	7.7 ± 2.2	8.8 ± 1.7	7.7 ± 1.8	7.7 ± 2.2	8.6 ± 3.0	7.5 ± 1.8
{10$\bar{1}$2} and {01$\bar{1}$2}	—	—	7.4 ± 1.1	6.8 ± 1.2	7.3 ± 1.2	8.6 ± 1.5	6.1 ± 1.2	5.8 ± 1.2	5.7 ± 1.6	6.0 ± 0.96
{10$\bar{1}$1} and {01$\bar{1}$1}	—	8.4 ± 1.4 15 ± 4.0	8.4 ± 2.2	8.2 ± 2.8	7.7 ± 1.8	11.0 ± 2.4	6.9 ± 1.1 17 ± 3.4	8.3 ± 3.8	8.4 ± 7.0	7.5 ± 1.1 19.1 ± 4.6
{2131}	—	—	8.4 ± 1.9	8.7 ± 2.5	7.4 ± 1.2	10.0 ± 1.4	6.7 ± 0.94	8.5 ± 4.2	9.6 ± 3.5	7.9 ± 1.3

Table 7 contains measurements of the distances between individual planes of multiple sets. The irregularity of the spacing is illustrated by the high values of standard deviation. Planar structures parallel to {0001} have the longest distances. Sets parallel to {10$\bar{1}$3} and {10$\bar{1}$2} display the most uniform pattern. {10$\bar{1}$1} shows in some cases a bimodal distribution of distances.

If viewed parallel, the individual planes of multiple sets of planar structures appear in most cases as very straight, extremely plane parallel lines. However if they are not too closely spaced, some deviations from parallelism become obvious as illustrated in Fig. 14. These tilted elements may have been produced by an "en echelon" combination of numerous very small elements, parallel to the principal plane of the set.

An other peculiarity is continuous bending of multiple sets of planar elements or lamellae. Examples are shown in Figs. 15 and 16. This bending demonstrates that slip occurred parallel to the planes of these structures. In the investigated samples, {10$\bar{1}$3} or {01$\bar{1}$3} are the most prominent slip planes. In some cases the slip along such planes can directly be observed by slight displacements of other planar elements crossing the first ones. An example is shown in Fig. 5.

3.4. Densities and Optical Properties of Ries Quartz with Planar Deformation Structures

Quartz with planar deformation structures has considerably lower density, refractive indices and birefringence than normal quartz. This is shown in Table 8, including refractive indices and densities for two diaplectic quartz glasses (B 41 and B 75).

Density and optical properties were measured on isolated grains, handpicked after the rock was crushed and fractioned with a magnetic separator. Grains with the optic axis nearly perpendicular to the microscope axis were used to determine refractive indices by immersion in mixtures of α-monobromnaphthalene and butyleneglycole. Thus the lower index measured corresponds to n_o, the higher approximates n_e. Accuracy was ± 0.0005. Fifty grains have been measured per sample.

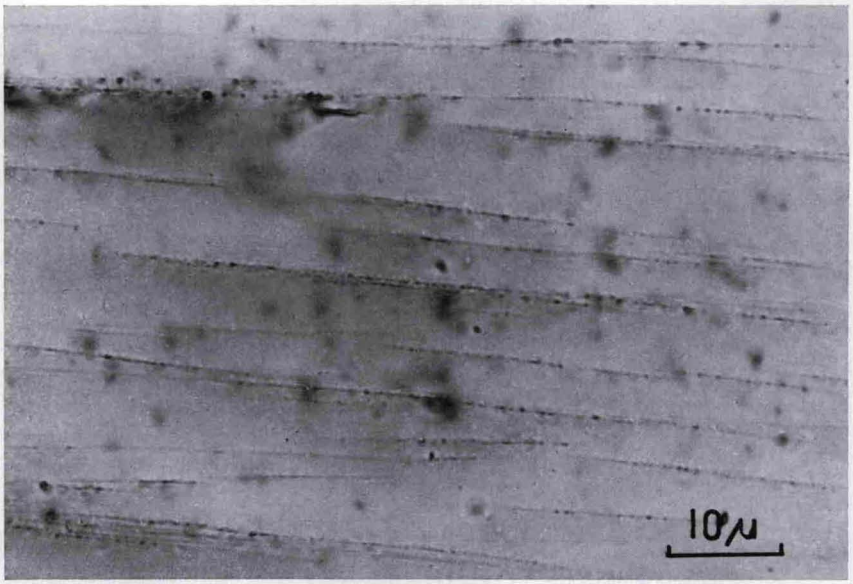

Fig. 14. Deviation from parallelism within multiple sets of planar elements parallel to $\{10\bar{1}3\}$. Quartzes from sample B 51. Normal light

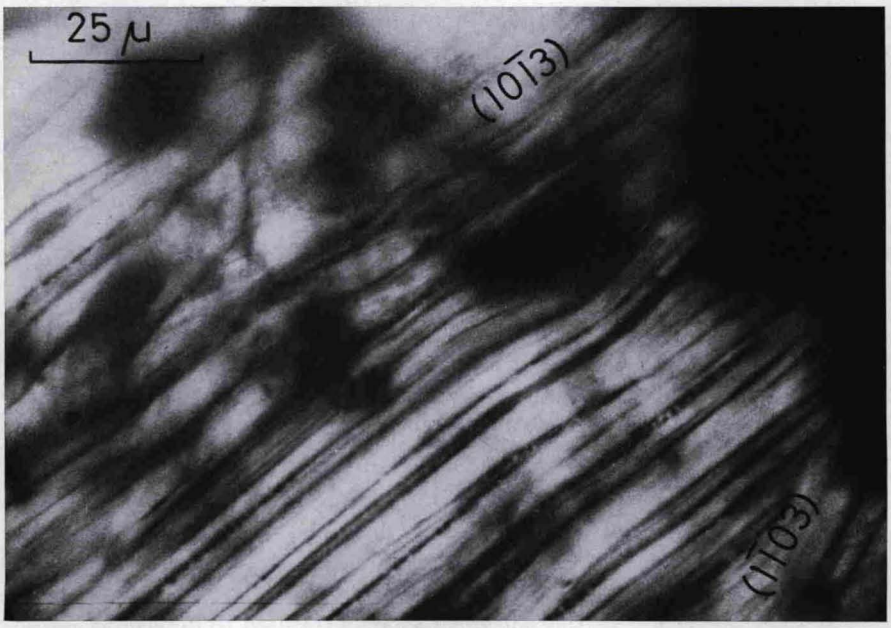

Fig. 15. Bending of filled lamellae. Quartz from sample S 289. Crossed nicols

The densities of 50 grains for each sample were determined by floating techniques (mixtures of bromoforme and dimethyleneformamide, accuracy was ± 0.001 g/cm^3).

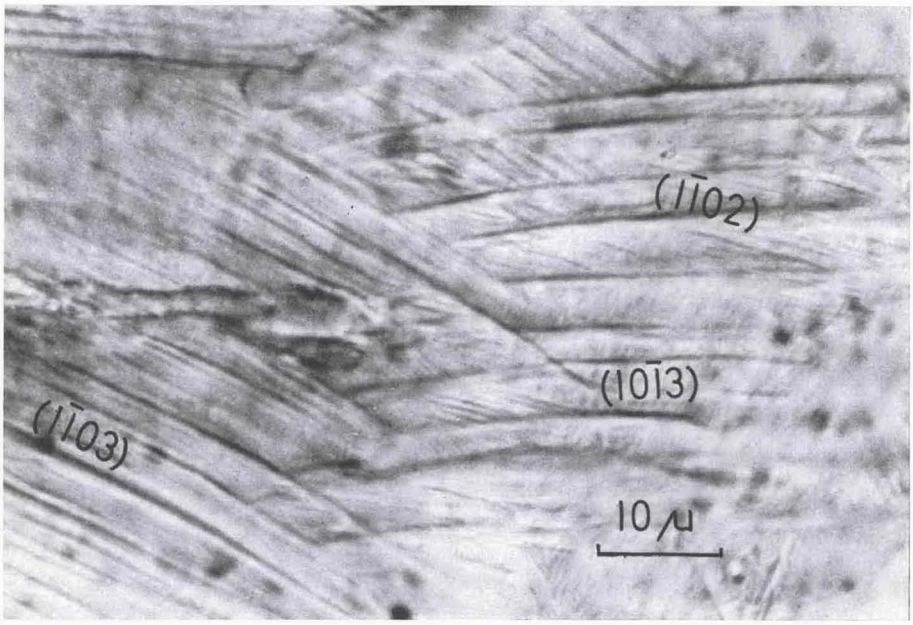

Fig. 16. Bending of non-decorated planar elements. Quartz from sample B 9. Plane polarized light

Table 8. *Refractive indices, birefringence and density of quartzes with planar deformation structures and of diaplectic quartz glasses (B 41, B 75)*

Sample	n_o		n_e (approx.)		n_e-n_o (approx.)	Density	
	range	mean	range	mean		range	mean
B 10	1.544—1.541	1.543	1.552—1.550	1.551	0.007	2.640—2.656	2.648
B 51	1.544—1.541	1.543	1.552—1.550	1.551	0.007	2.639—2.655	2.647
S 289	1.542—1.540	1.541	1.549—1.547	1.548	0.007	2.622—2.652	2.637
B 151	1.534—1.532	1.533	1.541—1.538	1.540	0.007	2.570—2.626	2.598
S 350	1.532—1.528	1.530	1.539—1.535	1.537	0.007	2.570—2.596	2.583
B 1	1.533—1.530	1.532	1.539—1.535	1.537	0.005	2.559—2.592	2.577
B 7[a]	1.480—1.475	1.478	1.485—1.480	1.483	0.005	2.256—2.296	2.276
B 9[a]	1.478—1.474	1.476	1.483—1.478	1.481	0.005	2.243—2.282	2.263
B 41	1.466—1.465	1.466	—	—	—	2.216—2.251	2.234
B 75	1.460	1.460	—	—	—	2.206—2.236	2.222

[a] The values of density and refractive indices are probably influenced by a small content of secondary recrystallisation products (clay mineral).

According to refractive index and density, the investigated quartz samples form a sequence, ranging from normal quartz down to diaplectic quartz glass: quartz from B 10 and B 51 is still very close to normal quartz ($d = 2.65$; $n_o = 1.544$; $n_e = 1.553$). On the other hand, quartz from B 7 and B 9 closely resembles the completely isotropic glasses from B 41 and B 75.

X-ray powder diagrams show in all optically anisotropic samples quartz lines with only minor deviations from the normal values of lattice constants[1]. It must consequently be assumed that all quartz samples of low densities and refractive indices are actually mixtures of crystalline quartz with an amorphous phase. The measured densities and indices are bulk values of truly heterogeneous grains, the heterogeneity being in a microscopical or submicroscopical scale. The presence of planar structures under the microscope does not contradict this assumption. In fact we assume, that all planar structures — but the genuine planar fractures — have to be interpreted as fine lamellae of amorphous SiO_2 embedded in a matrix of crystalline quartz. Thus they are actually responsible for the heterogeneity.

The higher the frequency of planar structures in a quartz grain, the larger is the amount of quartz transformed into an amorphous phase and the lower are bulk density and refractive index, finally resulting in a X-ray amorphous and optically isotropic diaplectic quartz glass. As shown in a previous paper (ENGELHARDT et al., 1967) these diaplectic quartz glasses are different from normal quartz glass: in general their indices of refraction and densities are higher. The observed range of densities was between 2.219 and 2.261 and that of refractive indices between 1.460 and 1.464 (normal quartz glass: $d = 2.20$, $n = 1.459$).

For reason of simplicity the amorphous phase in quartz with planar structures is assumed to have the properties of normal SiO_2-glass and the crystalline phase to be identical with normal quartz. The amount of glass present can then be calculated on the basis of the measured densities and refractive indices: Using the measured density d one obtains the volume percentage x_d of quartz glass as follows:

$$x_d = \frac{2.65 - d}{0.45} \cdot 100.$$

From the measured refractive index n_o one obtains

$$x_n = \frac{1.544 - n_o}{0.085} \cdot 100.$$

Calculated values are recorded in Table 9. The agreement between x_d and x_n is good. Therefore it is reasonable to calculate an average value $\bar{x}$ for the percentage of amorphous SiO_2 enclosed in the individual "quartz". These values are lower limits because the amorphous SiO_2 is a diaplectic glass having higher density and indices of refraction than the values used for these calculations.

Table 9. *Content of amorphous SiO_2 in quartzes with planar structures. Volume percentages as calculated from density (x_d) and index of refraction (x_n)*

Sample	x_d (%)	x_n (%)	Average $\bar{x}$ (%)
B 10	0.6	1.2	0.9
B 51	0.7	1.2	0.9
S 289	3	3	3
B 151	12	13	12
S 350	15	18	16
B 1	16	14	15
B 7[a]	82	78	80
B 9[a]	86	80	83

[a] See note, Table 8.

4. Comparison with Other Planar Deformation Structures

4.1. Böhm lamellae as Traces of Tectonic Quartz Deformation

Planar structures in quartz have been frequently observed in tectonites. For the purpose of this synopsis all may be called Böhm lamellae, although BÖHM (1883),

1. BUNCH (1968), CHAO (1968) and HÖRZ (personal communication 1968) report differences between shocked and normal quartz in lattice dimensions (larger cell) and X-ray intensities.

one of the first investigators, did not exhaustively describe all types of tectonic quartz deformation structures later found. For pioneering studies see ZIRKEL (1893). A compilation of the literature up until 1959 is given by CHRISTIE and RALEIGH (1959).

Böhm lamellae appear in thin sections as fine striae or lamellae which are darker or different in brightness from the surrounding quartz. The following description by CHRISTIE and RALEIGH (1959) summarizes the numerous observations of previous authors:

"They are narrow, subplanar structures which occupy a part or the complete area of a grain and generally are only found with one orientation in any grain. They are not all structurally similar when seen under the highest magnification available: some consist entirely of minute brownish inclusions concentrated in planar zones; others cannot be resolved into individual inclusions and apparently have a different refractive index from the host grain; still others, intermediate between these two types, show a slight difference of refractive index and yet appear to consist in part of planes of inclusions. Although the lamellae are gently undulating they may all be measured by the U-stage . . . Many of the lamellae have an extinction position which is slightly but markedly different from that of the neighboring part of the host grain. These lamellae are very conspicuous between crossed Nicols, particularly when the grain is closely to the extinction position. The differences in the extinction position between lamellae and host grain are generally less than 3°." The brownish inclusions are supposed to be cavities filled with gas or liquid.

Somewhat similar to Böhm lamellae are deformation bands which are considerably broader than lamellae and bounded by fractures which are not distinclty planar and the orientation of which cannot be accurately measured. Lamellae and deformation bands occurring in the same grain, are parallel and have probably the same origin (WEISS, see CHRISTIE and RALEIGH, 1959).

Böhm lamellae are arranged in parallel sets which do not transgress grain boundaries. Most commonly one set per grain exists, rarely more than two. The individual planes are not exactly parallel to each other and generally they show a wave-shaped bending. Very often zones of undulatory extinction extend perpendicular to these planes, indicating that gliding occurred parallel to the planes of Böhm striation combined with folding (undulatory zones).

Recently CARTER and FRIEDMAN (1965) gave a different description of quartz lamellae observed in a folded calcite-cemented sandstone. In this particular rock three types of deformation lamellae were distinguished:

Type I. In bright field illumination: fuzzy platelets or lenticles, 0.5 to 2 microns thick, brighter than the host quartz when in focus, extinguishing within less than one degree of rotation from the adjacent quartz. In phase contrast illumination they are much more prominent when the incident light vibrates parallel to n_e of quartz rather than n_o, characterized by a sharp planar discontinuity, being dark on one side respectively brighter on the other, thus indicating higher indices and birefringence than the host quartz on one side (dark side) of the discontinuity and lower indices and birefringence on the other side.

Type II consists of very minute brownish cavities or inclusions, showing little or no change in indices of refraction or birefringence.

Type III is intermediate between I and II. Differences in indices of refraction and birefringence between lamellae and host quartz appear to decrease with increasing numbers of the cavities or inclusions.

All investigators of Böhm lamellae agree to attribute them to gliding processes caused by tectonic stress. Investigations by Christie and Raleigh (1959), Naha (1959), Hansen and Borg (1962), Scott, Hansen and Twiss (1965), Carter and Friedman (1965) and others confirmed earlier studies that a strong relation exists between the orientation of quartz lamellae and the principal stress axes of the deformed rocks.

The planes of Böhm lamellae cluster parallel to planes of maximum resolved shear stress. They are most abundant in planes inclined at slightly smaller angles than 45° to the axis of maximum compressive stress. The lamellae are interpreted as

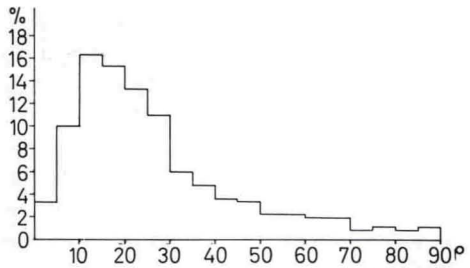

Fig. 17. Böhm lamellae. Frequency distribution of 3835 measured angles between normals to Böhm lamellae and c-axis of quartz grains from seven different sources, measured by several authors. (After Carter and Friedman, 1965)

traces of slip causing internal rotation either of the entire quartz grain or most commonly of confined domaines. These zones have been rotated with respect to the surrounding crystal and appear as zones of undulatory extinction or when sharply confined as deformation bands. Because most lamellae are inclined at small angles to (0001), slipping tends to move the c-axis of quartz towards the axis of maximum compressive stress.

Fig. 17 shows the frequency distribution of 3835 measured angles between the quartz c-axis and normals to Böhm lamellae, according to a compilation of Carter and Friedman (1965) summarizing the results of seven investigations of various rock types (Christie and Raleigh, 1959; De, 1958; Saha, 1955; Ingerson and Tuttle, 1945; Fairbairn, 1941; Hansen and Borg, 1962; Carter and Friedman, 1965).

Most lamellae are inclined at angles between 10 and 30° to the optic axis, a prominent maximum being between 10 and 20°. There is considerable uncertainty as to the degree of crystallographic control of the Böhm lamellae. Fischer (1925) and earlier investigators assumed orientation parallel to (0001), (10$\bar{1}$1), (01$\bar{1}$1) and flatter rhombohedra. Sander (1930) attributed his lamellae to (10$\bar{1}$3) and (10$\bar{1}$2). Hietanen (1938) considers gliding along (0001) and rupturing parallel to c as the responsible process for quartz deformation in Finnish quartzites. Though occasionally particular sets can be identified with low index lattice planes of quartz, no crystallographic quartz plane matches with the 10—20° maximum of Böhm lamellae (Fig. 17). Furthermore, the smooth frequency distribution of lamellae poles without prominent peaks presents no convincing evidence for any crystallographic control.

Some investigators (FAIRBAIRN, 1941; INGERSON and TUTTLE, 1945; CHRISTIE and RALEIGH, 1959), emphasized therefore that Böhm lamellae have not to be parallel to rational lattice planes. FAIRBAIRN (1941) suggested gliding along a fixed direction, presumably the edge between rhombohedron and prism face, however in varying glide planes. CHRISTIE and RALEIGH (1959) proposed that Böhm lamellae are kinkbands (deformation lamellae) produced by gliding parallel to c: Kinking is assumed to occur along irregular surfaces inclined at high angles to c which are oriented such that there is high resolved shear stress suitable for gliding parallel to c.

The diagnostic characteristics of Böhm lamellae by which they can be distinguished from planar structures found in quartz from Ries rocks and from other suspected meteoritic craters can be summarized in the following way:

Böhm lamellae

(1) are not necessarily parallel to rational lattice planes and prefer an inclination of 10—20° to (0001),
(2) show nearly always an undulatory trend (bending),
(3) are very often not strictly parallel to each other,
(4) are always connected with zones of undulatory extinction,
(5) occur mostly in one and rarely in more than two sets per grain,
(6) show a distinct geometrical relationship between their fabric and the principle stress axes of the deformed rock.

4.2. Planar Structures Produced in Experiments under Static High Pressure Conditions

Earlier investigations of mechanical deformation of quartz at room temperature and pressures up to 30 kbar indicated only brittle fracture without evidence of plastic flow (CHRISTIE, HEARD, LA MORI, 1964). But application of higher temperatures (500—900° C) and confining pressures between 15 and 20 kbar resulted in plastic flow of single quartz crystals and polycrystalline materials (CHRISTIE, GRIGGS, CARTER, 1964; CARTER, CHRISTIE, GRIGGS, 1964).

Their recovery products displayed truly microscopic planar structures. CHRISTIE, GRIGGS and CARTER (1964) distinguished the following four principal types:

(1) Deformation lamellae: narrow, closely spaced planar or lenticular features, occurring in parallel sets, terminating inside the individual grain boundaries and extinguishing exactly or very close with the adjacent quartz. Commonly, the lamellae are approximately normal to zones of undulatory extinction. In plane polarized light, the lamellae show greatest relief (which appears to be negative on the basis of Becke line effects) when the vibration direction is parallel to n_e. In bright field illumination the lamellae have the appearance of thin bands 1—2 μ thick with an index of refraction and a birefringence slightly less than that of the host quartz. When the microscope is focussed on the upper surface of the thin section, they appear brighter than the host quartz and are flanked by fuzzy dark regions. In phase-contrast illumination the lamellae are asymmetric — dark on one side and bright on the other. It is concluded that the lamellae are comprised of a region higher index on one side of a sharp discontinuity, respectively, and

lower index of refraction on the other side. This variation in refractive index in the immediate vicinity of lamellae is associated with a variation in birefringence, one side having a higher, the other side a lower birefringence than the host. Each region of abnormal index decays within a very short distance into the index of the host quartz. The asymmetric nature of these lamellae is also confirmed by microphotographs using a two-ray-interference-microscope (own observation).

The poles of the lamellae are nearly symmetrically distributed around and angle of 45° to the direction of maximum compression, the lamellae, therefore originating in planes of maximum resolved shear stress.

In quartzite samples most lamellae are parallel or subparallel to (0001), the poles forming angles between 0 and 10° to c (maximum between 2 and 6°). The poles of other lamellae cluster between 20 and 60° to c.

The development of deformation lamellae in single crystals depends heavily on the orientation of the crystal lattice to the axes of stress. Deformation lamellae parallel to (0001) are most readily formed, when compressed in a direction perpendicular to $(10\bar{1}1)$. Closely spaced sets of this orientation are produced if shear stress on the basal plane is high. In crystals of the same orientation there are also lamellae parallel to one of the prism faces. Other lamellae have been identified with $\{10\bar{1}1\}$, $\{11\bar{2}2\}$ and $\{10\bar{1}2\}$ (Christie and Green, 1964).

The deformation lamellae parallel or subparallel to (0001) have been extensively investigated by Christie, Griggs and Carter (1964). The lamellae are interpreted to be caused by slip in the (0001)-plane along the a-axis. It was shown that the optical asymmetry is consistent with photoelastic effects which would be expected from an array of edge dislocations of Burgers vektor $\vec{b} = \vec{a}$ in the basal plane. Calculations of the stress field due to such an array show that a dislocation density of $8 \cdot 10^4$ cm^{-1} per lamella is required to produce the observed optical effects. The validity of this model was supported by electron micrographs of replicas of etched polished surfaces of crystals with such deformation lamellae. Pyramidal etch pits the density of which varied from $5 \cdot 10^4$ to $13 \cdot 10^4$ cm^{-1} were observed in rows parallel to the trace of (0001).

Further studies applying transmission electron microscope technique (McLaren Retchford, Griggs and Christie 1967) revealed that basal slip produces narrow Brazil twin bands parallel to (0001) and that the nature of the dislocations is either of pure screw type ($\vec{b} = \vec{a}$ [10.0]) or of a particular mixed character, predominately edge type with a 30° screw component.

Minor deviations of lamellae from (0001) are explained by Christie, Griggs and Carter (1964) by two possible mechanisms: (1) some lamellae may originate as "en echelon" arrays of basal dislocations locked in different slip planes. (2) lamellae being either initially parallel to the base or consisting of en echelon arrays may be internally rotated by slip on some other system.

(2) Extension fractures: are short, lenticular features which occur in subparallel sets. They invariably terminate within grain boundaries and are generally shorter and less continuous than the deformation lamellae. Their inclination in thin sections cannot be determined as accurately as that of lamellae. In the plane normal to the thin section they have strongly lenticular profiles. They are not associated

with undulatory extinction nor extinction bands. They occur parallel to planes of low shear stress, usually normal but occasionally parallel to the direction of maximum compressive stress. According to CARTER, CHRISTIE and GRIGGS (1964) they are open extension fractures produced during unloading of the samples.

(3) Undulatory extinction: A continuous gradation between deformation bands and undulatory extinction exists, both involving reorientation of the quartz structure by bending. If bending has taken place with a radius of curvature comparable with or larger than the half-width of the reoriented zone, the feature is designated undulatory extinction. Undulatory extinction in the experimentally deformed quartz samples most commonly occurs in zones subparallel to c, as it is known from undulatory extinction in naturally deformed quartz. Therefore, undulatory extinction is connected with bending of basal planes. The maximum observed difference in the orientation of adjacent c-axes is 12°, a value which corresponds to undulatory extinction known from naturally deformed quartz.

(*4*) *Deformation bands*: are generally less than 0.05 mm wide. They may occur as single individuals, however parallel sets are more common. Few grains may contain two sets of bands. The angles between c-axes of band and host grain vary between 3 to 25°, the average being about 10°. Generally the poles of band boundaries define two maxima at about 45° to the direction of maximum compressive stress, indicating that the bands formed in planes of high shear stress. The angles between poles of the band boundaries and the c-axes in the host grain may vary considerably, but most frequent the bands are parallel or subparallel to the c-axis: two thirds of the bands are inclined less than 20°, one half less than 10° to the c-axis. For bands subparallel to the c-axis the pole of the band, the c-axis in the host grain and the c-axis in the band commonly lie in a plane parallel to the direction of maximum compressive stress. The direction of rotation of the c-axis from the host to the band is most commonly towards this direction. Deformation lamellae that are approximately parallel to the base are present in all bands subparallel to the c-axis.

Deformation bands are interpreted by CHRISTIE, GRIGGS and CARTER (1964) to be kink bands originating by slip on the basal plane along the a-axes. Undulatory extinction in zones subparallel to the c-axis is similar to the kink bands and probably results from bending and gliding along the basal slip planes.

4.3. Planar Structures Produced in Experiments under Dynamic High Pressure Conditions

Within the last years several investigators successfully reproduced planar deformation structures by shock loading quartz bearing rocks, polycrystalline quartz or single quartz crystals (MILTON et al., 1961; SHORT, 1966a, b, c; FRYER, 1966; MÜLLER and HORNEMANN, 1967). SHORT (1966a) observed planar structures parallel to $\{10\bar{1}3\}$ in quartz of a granodiorite from an underground nuclear explosion. A range of 50 to 75 kbar was estimated as the lower limit of shock wave peak pressure necessary for the formation of these planar deformation structures. Using explosives SHORT (1966c) obtained planar structures parallel to $\{10\bar{1}3\}$ at estimated peak pressures between 75 and 175 kbar and between 300 and 400 kbar.

Recently controlled shock wave experiments with exactly known pressures in the range of 50 to 600 kbar have been performed by Müller and Defourneaux (1968), Müller and Hornemann (1968) and Hörz (1968). These investigations resulted in the following information about shock induced deformation features in quartz:

~50 — ~100 kbar: characteristic for the lower pressure range are planar fractures parallel to {0001}, {10$\bar{1}$1} and {10$\bar{1}$0}. They form in planes of high resolved shear stress: in experiments with single crystals, shock waves propagating perpendicular to {0001} and {10$\bar{1}$0} generate primarily planar fractures parallel to {10$\bar{1}$1} whereas impacts parallel to {10$\bar{1}$1} produce fractures parallel to {0001} and {10$\bar{1}$0}. These fractures appear under the microscope as comparatively broad features, 2—10 μ thick and mostly 20 μ or more apart from each other.

~100 — ~380 kbar: besides the before mentioned structures, planar elements of the non-decorated type are formed which appear as planar optical discontinuities arranged in closely spaced (2—5 μ apart) multiple sets of crystallographic orientation. The shocked grains have a tendency to break along these elements. They are not resolved, even with highest magnification. Hörz (1968) observed very few (~ 1%) features of the type named "deformation lamellae" by Christie, Griggs and Carter (1964). In general, no asymmetry was found in bright field and in phase contrast illumination. Some planar elements appear to be lamellae of a finite width of about 1—2 μ. The first planar elements to appear at pressures above about 120 kbar are parallel to {10$\bar{1}$3}. At pressures between 160 and 200 kbar planar elements parallel to {10$\bar{1}$2} appear. They become more frequent than those parallel to {10$\bar{1}$3} at pressures exceeding about 280 kbar. The spacing of {10$\bar{1}$2} elements is closer than that of {10$\bar{1}$3} elements. Less prominent are planar elements parallel to the following crystallographic planes: {0001}, {10$\bar{1}$1}, {11$\bar{2}$2}, {21$\bar{3}$1}, {51$\bar{6}$1}, {11$\bar{2}$1} (Hörz), {10$\bar{1}$0} (Hörz), {22$\bar{4}$1} (Müller and Defourneaux).

At pressures of 260—280 kbar Müller and Defourneaux (1968) observed in single crystals of quartz the formation of deformation bands with diffuse boundaries inclined at 45—60° against the c-axis of the host. The angle between the c-axes of band and host was about 10°. The bands contain planar structures perpendicular and parallel to the band boundaries and are sometimes markedly bent.

Optical properties and density of the deformed quartz remain nearly unchanged below shock wave pressures of about 200 kbar. At higher pressures refractive indices, birefringence and density are markedly lowered, the decrease becoming most prominent at pressures of 280—300 kbar. In this range mean refractive index declines below 1.50, birefringence below 0.004 and density to 2.27 g/cm^3.

At pressures of about 300kbar the first small patches of isotropic diaplectic quartz glass start to form. Larger amounts of diaplectic glass ($n = 1.460$) have been observed in experiments at about 380 kbar.

Peak pressures of 500 to 600 kbar produced normal fused quartz glass with $n = 1.459$ (Müller and Hornemann, 1968).

In experiments with untwinned single crystals Müller and Hornemann (1968) have found that shock waves propagating in the directions [11.0], [21.0] and [10.0] produced planar structures exclusively parallel to {10$\bar{1}$3} and {01$\bar{1}$2}, but not parallel to {01$\bar{1}$3} and {10$\bar{1}$2}.

5. Discussion

Planar structures observed in quartz of various Ries rocks can be distinguished from deformation structures in tectonites (Böhm lamellae) and those produced in static high pressure experiments (low strain rate) by the following features:

(1) The development of planar structures is stronger controlled by the crystal structure of quartz.

(2) $\{10\bar{1}3\}$ and $\{10\bar{1}2\}$ are more frequent than $\{0001\}$.

(3) There are more sets of planar structures per grain.

(4) In general, the planar structures are sharper, more plane parallel, more closely spaced.

(5) Lamellae with optical asymmetry in phase contrast illumination (deformation lamellae of CARTER, CHRISTIE and GRIGGS) are very rare or even absent.

(6) Grains with planar deformation structures show lower bulk values of density, refractive index and birefringence, indicating that deformation was connected with partial destruction of the crystal lattice of quartz.

(7) In contrast to Böhm lamellae and planar structures produced experimentally under static conditions, the planar structures in quartz bearing Ries rocks show no relation to general direction of stress within the rock (e.g. planes of maximum resolved shear stress), because of the disorganisation of a shock wave travelling through a heterogenous rock (RINEHART, 1968).

Apart from the decoration by minute bubbles or inclusions — not reproduced in shock experiments as to date — the planar structures of Ries quartz are most similar to the deformation features obtained experimentally under shock conditions with peak pressures in the order of 100 to 380 kbar. Apparently the natural and artificial planar structures of this kind are traces of plastic flow, following under the high strain rates and pressures within a shock wave other glide planes as compared to static conditions and lower pressures.

The arrangement of the planes observed in zones (see Fig. 10) seems to indicate that the vectors $\vec{a}_1 = [10.0]$ (length = 4.913 Å), $2\vec{a}_1 + \vec{a}_2 = [21.0]$ (length = 8.510 Å) and $\vec{a}_1 + \vec{c} = [10.1]$ (length = 7.303 Å) are probably the principal glide directions.

The most frequent glide planes contain the shortest Bravais vector of the quartz lattice, $\vec{a}_1$: $\{0001\}$, $\{10\bar{1}3\}$, $\{10\bar{1}2\}$, $\{10\bar{1}1\}$, and $\{10\bar{1}0\}$. When the peak pressure exceeds about 120 kbar, gliding parallel to $\{10\bar{1}3\}$ or $\{01\bar{1}3\}$ is favoured over basal gliding, the typical process at lower stresses and under static conditions. At higher stresses ($> \cong 180$ kbar) or when slip parallel to $\{10\bar{1}3\}$ or $\{01\bar{1}3\}$ has ceased due to work hardening or other impediments, additional gliding develops parallel to $\{10\bar{1}2\}$ or $\{01\bar{1}2\}$.

Of secondary importance are slip planes containing the vector $2\vec{a}_1 + \vec{a}_2$ like $\{11\bar{2}2\}$ and $\{11\bar{2}1\}$ and those parallel to the vector $\vec{a}_1 + \vec{c}$ like $\{51\bar{6}1\}$ and $\{21\bar{3}1\}$.

Shock experiments with single quartz crystals by MÜLLER and HORNEMANN (1968) yielded noticeable differences in the case of developing glide systems parallel to positive and negative rhombohedra of the same index: planar structures parallel to $\{10\bar{1}3\}$ or $\{01\bar{1}2\}$ are more readily formed than those parallel to $\{01\bar{1}3\}$ and $\{10\bar{1}2\}$, respectively. This result is in accordance with the observation that Ries

quartz containing planar elements parallel to the above rhombohedra display preferably combinations of alternating positive and negative forms (see p. 217). A structural reason for the preference of $\{10\bar{1}3\}$ over $\{01\bar{1}3\}$ respectively $\{01\bar{1}2\}$ over $\{10\bar{1}2\}$, is probably the sequence of atomic planes. Both $\{10\bar{1}3\}$ and $\{0\bar{1}12\}$ contain two Si planes following each other without an O plane between them, in contrast to $\{01\bar{1}3\}$ and $\{10\bar{1}2\}$, containing sequences of planes of the type Si-O-Si, as illustrated in Fig. 18. The configuration of next neighbour Si planes may perhaps be favourable for gliding under shock conditions. Neither $\{10\bar{1}1\}$ nor $\{01\bar{1}1\}$

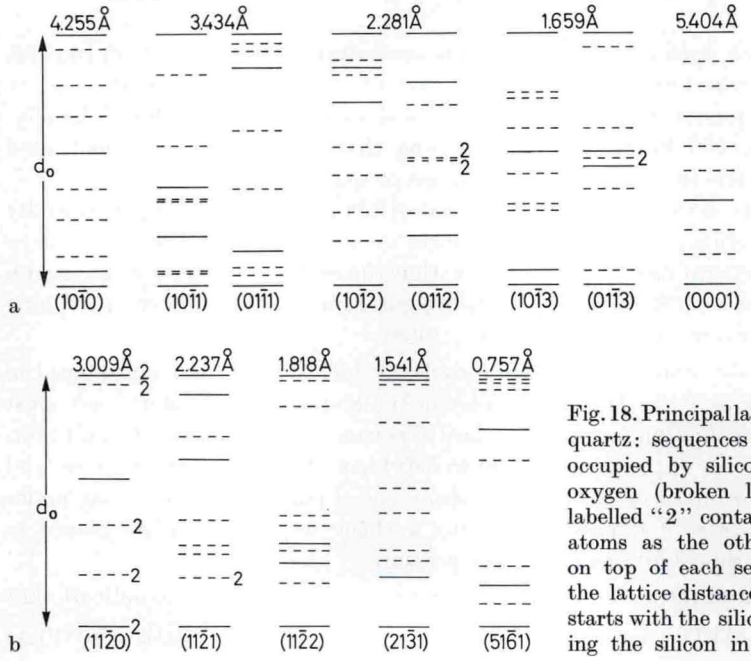

Fig. 18. Principal lattice planes of low-quartz: sequences of atomic planes occupied by silicon (full line) and oxygen (broken line). The planes labelled "2" contain twice as much atoms as the other ones. Figures on top of each sequence designate the lattice distances. Each sequence starts with the silicon plane containing the silicon in position [|u00|]

contains such a configuration. However, it exists for $\{10\bar{1}0\}$ as well as $\{11\bar{2}1\}$ and $\{21\bar{3}1\}$. $\{0001\}$, $\{11\bar{2}0\}$, $\{11\bar{2}2\}$ and $\{51\bar{6}1\}$ planes do not contain immediately opposed Si planes.

The most characteristic properties of shocked quartz, however, are their reduced densities, refractive indices and birefringences. These effects become obvious in the laboratory at peak pressures exceeding about 200 kbar. The change of physical properties indicates that shock waves of sufficient pressures not only cause plastic and ruptural deformation but also produce irreversible transformation of the quartz lattice.

The Hugoniot curves obtained by Wackerle (1962) and Ahrens and Rosenberg (1968) from shock experiments with quartz indicate for both single crystal and polycrystalline quartz a greater compression rate above about 120 kbar as one would expect from the compressibility of quartz determined by Bridgeman (1948) at lower pressures. The same stress limit (Hugoniot elastic limit) defines according to the experiments of Hörz (1968) and Müller and Defourneaux

(1968) the begin of plastic flow under shock conditions as revealed by the first appearance of planar structures in the recovered material. The higher compressibility above about 120 kbar is interpreted by AHRENS and ROSENBERG (1968) to be due to a partial transformation to one of the high pressure polymorphs of SiO_2, either coesite or stishovite. Between 300 and 370 kbar both the single crystal and polycrystalline quartz Hugoniots rapidly approach the pressure/volume curve that is apparently characteristic for stishovite (MCQUEEN et al., 1963). Release adiabates measured by AHRENS and ROSENBERG (1968) indicate that the material produced by shock waves at pressures between the elastic limit and about 380 kbar is either a mixture of quartz and coesite or quartz and stishovite, which is retained, at least momentarily, at zero pressure. These concluisons were drawn from the volume/pressure relationship, without investigating recovery products. The experiments of HÖRZ (1968) and MÜLLER and DEFOURNEAUX (1968) yielded material of the same or lower densities and indices of refraction than normal quartz, confirming the observations on Ries quartz. Consequently we and HÖRZ (1968) assume that the high pressure phases formed in the shock front are rapidly transformed upon release into a glass (diaplectic glass) with density and index of refraction close to fused SiO_2-glass. It is probably safe to assume that, only minor amounts — if any — of high pressure phases have been recrystallized to quartz. Under the assumption that also the diaplectic glass was not transformed into quartz, the quartz content of shocked quartz is identical with the quantity of quartz that survived the shock unaffected. This quantity decreases with increasing shock pressure and becomes zero at about 400 kbar pressure level at which the material after relase consists entirely of diaplectic glass. Bulk refractive indices and densities of shocked quartz or the amounts of crystalline quartz calculated from these data (Table 9) may be used as a measure of shock intensity in the 200 to 400 kbar range. Since the shock damaged quartz bearing rocks from the Ries are listed in Table 1 in order of decreasing mean refractive index of quartz, this order approximately represents a series of rock samples subjected to shock waves of increasing peak pressures.

Quartz deformation by shock waves as documented by quartz containing planar structures in the Ries breccias can be summarized as follows:

Under the influence of shock waves with peak pressures exceeding the Hugoniot elastic limit quartz behaves in a plastic manner and fails by gliding parallel to several lattice planes, predominately $\{10\bar{1}3\}$, $\{01\bar{1}2\}$, $\{10\bar{1}1\}$ or $\{01\bar{1}1\}$ and $\{0001\}$. Prior to plastic deformation and probably at lower stress levels planar fractures are formed, preferently parallel to $\{0001\}$ and $\{10\bar{1}1\}$. Simultaneously with gliding the quartz begins to transform into a high pressure modification, most probably stishovite or even a dense phase not yet perfectly ordered with six-fold coordination of oxygen around silicon. These phase transitions focus along glide planes with high shear strain and abundant lattice disturbations, caused by the accumulation of dislocations. These seem to be favorite conditions for the nucleation and formation of new phases. In this way thin lamellae of a dense phase are formed parallel to the numerous traces of glide planes dissecting the individual quartz grains. The amount of the new phase depends on the peak pressure of the shock wave. A total transformation is completed when the peak pressure reaches about 400 kbar. Under favourable circumstances

(rapid cooling ?) some stishovite can survive the pressure and temperature release as demonstrated by the stishovite rich rock S 289 from Appetshofen. But generally, during pressure and temperature release — eventually somewhat earlier — the dense phase breaks down resulting in a more disordered "diaplectic" SiO_2-glass with properties similar to but different from those of fused SiO_2-glass and some coesite[2]. If the transition to a high pressure phase was not complete, the final release products is "quartz" (diaplectic quartz) with planar structures, as remnant of gliding processes, with lower values of density, refractive index and birefringence, due to the coexistence of glassy and crystalline SiO_2. Quartz subjected to peak pressures close to 400 kbar is completely transformed into diaplectic glass (samples B 41 and B 75).

Two particular phenomena which are observed in the shock deformed Ries quartz are not yet fully understood: the homogeneous lamellae and the decoration of planar elements, as described in chapters 3.1.3. and 3.1.1.

Homogenous lamellae may be deformation bands (kink bands), but further investigations have to be carried out with samples containing outstanding structures of this kind.

The small bubbles or inclusions of decorated planar elements resemble those known from Böhm lamellae of tectonites. Several formation processes seem possible:
(1) Coagulation of atomic vacancies formed in the slip plane by non-conservative movement or mutual interaction of dislocations.
(2) Healing of originally open fractures
(3) Segregation of originally dissolved gaseous contaminants.

Decorated planar elements are most abundant in Ries rocks which experienced shock waves with peak pressures not too much above the Hugoniot elastic limit of quartz. Quartz with low densities and refractive indices like those from rocks B 7 and B 9, contain only non-decorated planar elements. Apparently the decorations can not be formed and/or preserved if the shock dammage of quartz has exceeded a certain degree.

Acknowledgements. This study would not have been possible without the cooperation of all members of the Mineralogical Institute, University of Tübingen, concerned in the study of shock metamorphism of natural materials. We are particularly grateful to Dr. D. Stöffler and Dr. W. F. Müller for many fruitful discussions and constructive suggestions.
We are most indebted to Dr. F. Hörz, Seismological Laboratory, California Institute of Technology, Pasadena and Dr. T. E. Bunch, Ames Research Center, NASA, Moffett Field (California) for careful reviewing the manuscript.

References

Ahrens, T. J., and J. T. Rosenberg: Shock metamorphism: experiments on quartz and plagioclase. Conference on shock metamorphism of natural materials, Greenbelt (April 14—16, 1966). In press 1968.

Böhm, A.: Über die Gesteine des Wechsels. Mineral. Petrogr. Mitt. **5**, 197—214 (1883).

Bridgeman, P. W.: The compression of 39 substances to 100000 kg/cm². Proc. Am. Acad. Arts Sci. **76**, 55—70 (1948).

Bunch, T. E., and A. J. Cohen: Shock deformation of quartz from two meteorite craters. Bull. Geol. Soc. Am. **75**, 1263—1266 (1964).

2. Another effect of pressure release are numerous irregular fractures (extension fractures) in the quartz grains which are obviously later than all planar structures.

Carter, N. L.: Basal quartz deformation lamellae, a criterion for recognition of impactites. Am. J. Sci. **263**, 786—806 (1965).
— J. M. Christie, and D. T. Griggs: Experimental deformation and recrystallization of quartz. J. Geol. **72**, 687—733 (1964).
— Dynamic deformation of quartz. Conference on shock metamorphism of natural materials, Greenbelt (April 14—16, 1966). In press 1968.
—, and M. Friedman: Dynamic analysis of deformed quartz and calcite from the Dry Creek Ridge anticline, Montana. Am. J. Sci. **263**, 747—785 (1965).
Chao, E. T. C.: Shock effects in cartain rock forming minerals. Science **156**, 192—202 (1967).
— Pressure and temperature histories of impact metamorphosed rocks — Based on petrographic observations. Neues Jahrb. Mineral., Abhandl. **108**, 209—246 (1968).
— Some aspects of progressive impact metamorphism. Conference on shock metamorphism of natural materials, Greenbelt (April 14—16, 1966). In press 1968.
Christie, J. M., and H. W. Green: Several new slip mechanisms in quartz. Trans. Am. Geophys. Union **45**, 103 (1964).
—, D. T. Griggs, and N. L. Carter: Experimental evidence of basal slip in quartz. J. Geol. **72**, 734—756 (1964).
— H. C. Heard, and P. N. La Mori: Experimental deformation of quartz single crystals at 27 to 30 kilobars confining pressure and 24° C. Am. J. Sci. **262**, 26—55 (1964).
—, and C. B. Raleigh: The origin of deformation lamellae in quartz. Am. J. Sci. **257**, 385—407 (1959).
De, A.: Observations on the deformation lamellae in quartz of four Indian tectonites (abs.). Trans. Am. Geophys. Union **39**, 512 (1958).
Dence, M. R.: A comparative structural and petrographic study of probable Canadian meteorite craters. Meteoritics **2**, 249—270 (1964).
— The extraterrestrial origin of Canadian craters. Annals N.Y. Acad. Sci. **123**, 941—969 (1965).
Engelhardt, W. v.: Neue Beobachtungen im Nördlinger Ries. Geol. Rundschau **57**, 165—188 (1967).
— J. Arndt, D. Stöffler, W. F. Müller, H. Jeziorkowski u. R. A. Gubser: Diaplektische Gläser in den Breccien des Ries von Nördlingen als Anzeichen von Stoßwellenmetamorphose. Contr. Mineral. and Petrol. **15**, 93—102 (1967).
— W. Bertsch, D. Stöffler, P. Groschopf u. W. Reiff: Anzeichen für den meteoritischen Ursprung des Beckens von Steinheim. Naturwissenschaften **54**, 198—199 (1967).
— F. Hörz, D. Stöffler, and W. Bertsch: Observations of quartz deformation in breccias of Clearwater Lake (Canada) and the Ries Basin (Germany). Conference on shock metamorphism of natural materials, Greenbelt (April 14—16, 1966). In press 1968.
—, and D. Stöffler: Spaltflächen in Quarz als Anzeichen für Einschläge großer Meteoriten. Naturwissenschaften **52**, 489 (1965).
—, — Stages of shock metamorphism in crystalline rocks of the Ries basin (Germany). Conference on shock metamorphism of natural materials, Greenbelt (April 14—16, 1966). In press 1968.
Fairbairn, H. W.: Deformation lamellae in quartz from the Ajibik formation, Michigan. Bull. Geol. Soc. Am. **52**, 1265—1278 (1941).
Fischer, G.: Mechanisch bedingte Streifungen an Quarz. Zentr. Mineral., Geol., Paläontol. A **1925**, 210—213.
French, B. M.: Sudbury structure, Ontario: Some petrographic evidence for an origin by Meteoritic Impact. Science **156**, 1094—1098 (1967).
Fryer, C. C.: Shock deformation of quartz sand. Int. J. Rock Mechanics and Mining Sci. **3**, 81—88 (1966).
Hansen, E., and I. Y. Borg: The dynamic significance of deformation lamellae in quartz of a calcite cemented sandstone. Am. J. Sci. **260**, 321—336 (1962).
Hietanen, A.: On the petrology of the Finnish quartzites. Bull. comm. géol. Finlande Nr. **122**, 1—118 (1938).
Hörz, F.: Statistical measurements of deformation structures and refractive indices in experimentally shock loaded quartz. Conference on shock metamorphism of natural materials, Greenbelt (April 14—16, 1966). In press 1968.

Ingerson, E., and O. F. Tuttle: Relations of lamellae and crystallography of quartz and fabric directions in some deformed rocks. Trans. Am. Geophys. Union **26**, 95—105 (1945).

McIntyre, D. B.: Impact metamorphism at Clearwater Lakes, Quebec (Abstract). J. Geophys. Research **67**, 1647 (1962).

McLaren, A. C., J. A. Retchford, D. T. Griggs, and J. M. Christie: Transmission electron microscope study of brazil twins and dislocations experimentally produced in natural quartz. Phys. Stat. Sol. **19**, 631—644 (1967).

McQueen, R. G., J. N. Fritz, and S. P. Marsh: On the equation of state of stishovite. J. Geophys. Research **68**, 2319—2322 (1963).

Milton, D. J., J. Littler, J. J. Fahey, and E. M. Shoemaker: Petrography of glassy ejecta from scooter 0,5-kiloton high explosive cratering experiment, Nevada. Astrogeol. Studies Progr. Rept. U.S. Geol. Surv. 88—92 (1961).

Müller, W. F., and M. Defourneaux: Deformationsstrukturen in Quarz als Indikator für Stoßwellen: eine experimentelle Untersuchung an Quarzeinkristallen. Z. Geophysik **34**, 483—504 (1968).

—, and U. Hornemann: Experimentelle Untersuchungen zur Wirkung von Stoßwellen auf Quarz und Feldspäte. 45. Jahrestag. der Dtsch. Mineralog. Ges., Berlin, 9. 10. 1967.

— — Personal communication 1968.

Naha, K.: Time of formation and kinematic significance of deformation lamellae in quartz. J. Geol. **67**, 120—124 (1959).

Preuss, E.: Das Ries und die Meteoritentheorie. Fortschr. Mineral. **41**, 271—312 (1964).

Rinehart, J. S.: Intense destructive stresses resulting from stress wave interactions. Conference on shock metamorphism of natural materials, Greenbelt (April 14—16, 1966). In press 1968.

Robertson, P. B., M. R. Dence, and M. A. Vos: Deformation in rockforming minerals from Canadian craters. Conference on shock metamorphism of natural materials, Greenbelt (April 14—16, 1966). In press 1968.

Saha, A. K.: Deformation lamellae in quartz from granophyric granite and diorite of Butgora-Sarjori area, eastern Singhbhum (abs.): Indian Sci. Congr. **42** nd, Calcutta, Proc. part 3, 184 (1955).

Sander, B.: Gefügekunde der Gesteine. Wien 1930.

Scott, W. H., E. Hansen, and R. J. Twiss: Stress analysis of quartz deformation lamellae in a minor fold. Am. J. Sci. **263**, 729—746 (1965).

Short, N. M.: (a) Effect of shock pressures from a nuclear explosion on mechanical and
— optical properties of granodiorites. J. Geophys. Research **71**, 1195—1215 (1966).
(b) Nuclear explosion induced microdeformation of rocks: an aid to the recognition of
— meteorite impact structures. Conference on shock metamorphism of natural materials, Greenbelt (April 14—16, 1966). In press 1968.
(c) Experimental microdeformation of rock materials by shock pressures from laboratory-scale impacts and explosions. Conference on shock metamorphism of natural materials, Greenbelt (April 14—16, 1966). In press 1968.

Stöffler, D.: Zones of impact metamorphism in the crystalline rocks of the Nördlinger Ries Crater. Contr. Mineral. and Petrol. **12**, 15—24 (1966).

— Deformation und Umwandlung von Plagioklas durch Stoßwellen in den Gesteinen des Nördlinger Ries. Contr. Mineral. and Petrol. **16**, 51—83 (1967).

—, and J. Arndt: Coesit und Stishovit, die Höchstdruckmodifikationen des Siliciumdioxids. Naturwissenschaften (1969) (im Druck).

Wackerle, J.: Shock compression of quartz. J. Appl. Phys. **33**, 922—937 (1962).

Zirkel, F.: Lehrbuch der Petrographie, 2. Aufl., S. 196. Leipzig 1893.

Prof. Dr. W. von Engelhardt
Mineralogisches Institut
7400 Tübingen, Wilhelmstr. 56